

INVESTIGATION OF EFFECTS OF CROSS-SECTIONS ON THE RAY-EFFECT DISTORTIONS

S. SAĞLAM¹

Abstract

In this study, a wellknown numerical method has been used to solve neutron transport equation and the ray-effect anomaly observed on the results of the method has been introduced. To examine the effects of cross-sections on the ray-effect, two Benchmark problems have been chosen as test problems. Then, two dimensional transport code, TWOTRAN-II has been executed for these problems for S_4 - S_{16} approximations. Finally, by comparing all the results with each other, the effects of cross-sections have been examined in detail.

1. INTRODUCTION

The main problem of reactor physics is determination of neutron distribution in a system; such as nuclear core. This is important because of the evaluation of different nuclear reactions. To determine distribution of neutrons, the process of neutron transport is investigated [1-2]. The neutron transport is given by neutron transport equation which states a mathematical balance on the physical production and losses of particles (Eg.1 and Eg.2).

$$\vec{L}\phi(\vec{r}, E, \vec{\Omega}, t) = Q(\vec{r}, E, \vec{\Omega}, t) \quad (1)$$

$$\vec{L} = \frac{1}{v} \frac{\partial}{\partial t} \vec{\Omega} \cdot \nabla + \sum_t(\vec{r}, E) - \int_{4\pi} d\vec{\Omega}' \int_0^\infty dE' \sum_s(\vec{r}, E' \rightarrow E, \vec{\Omega}' \rightarrow \vec{\Omega}) \\ - \chi(E) \int_{4\pi} d\vec{\Omega} \int_0^\infty dE' v(E') \sum_f(\vec{r}, E') \quad (2)$$

In nuclear reactor design and analysis, the solution of transport equation plays an important role. This solution consists of complete distribution of particles throughout the space, energy, direction of motion and time portions of the problem. However, it is very difficult to solve this equation, except for simple problems since it has an integro - differential form with seven variables. Other factors have also an effect complicating the solution, such as complex energy dependence of cross-sections and geometrical arrangement of materials used in the reactor. Therefore, the neutron transport equation together with the appropriate boundary conditions is solved usually by numerical solution methods. These methods may be probabilistic methods (i.e. Monte Carlo) or deterministic methods (i.e. P_N - spherical harmonics expansion method and S_N - discrete ordinates method [3-4]).

¹Istanbul University, Faculty of Science, Physics Department Vezneciler, İstanbul – TÜRKİYE

2. METHOD AND RAY-EFFECT

Discrete Ordinates Method, S_N , that is the main subject of this study is one of the important deterministic solution methods of neutron transport equation. The method is straightforward and widely used in transport calculations. In the method, a set of discrete directions (or ordinates) for angular variable is chosen and transport equation is evaluated for these directions by suitable averaging processes. The choice of these ordinates is not arbitrary; it seeks to satisfy some conditions [1,2], for example: they must satisfy certain mechanical integration requirements. The derivatives appearing in the equation are replaced by a corresponding discrete representation by using finite difference techniques (i.e. forward difference, diamond difference etc.) and the integrals in the equation are replaced by numerical integration schemes (i.e. standard Gauss quadratures: Gauss - Legendre quadrature (Eg. 3) and Gauss - Chebyshev quadrature (Eg.4)).

$$\int_{-1}^{+1} F(x)dx = \sum_{i=0}^n w_i F(x_i) \quad (3)$$

$$\int_{-1}^{-1} \frac{1}{\sqrt{1-x^2}} F(x)dx = \sum_{i=0}^n w_i F(x_i) \quad (4)$$

Where w_i are called as the weights of the quadratures.

In this study, the angular flux is expanded in a series of Legendre polynomials [4] as,

$$\phi = \sum_{n=0}^{\infty} (2n+1) \sum_{k=0}^n R_n^k \phi_n^k \quad (5)$$

and the expansion coefficients are given by,

$$\phi_n^k = \int_{-1}^{+1} d\mu \int_0^{\pi} d\varphi R_n^k \phi / 2\pi \quad (6)$$

The integral given above, according to the Gauss-Legendre quadrature consideration is approximated by the sum [4],

$$N_{nj}^k = \sum_{m=1}^{MT} w_m R_n^k(\mu_m, \varphi_m) N_{ijm} \quad (7)$$

Where, φ_m is defined in TWOTRAN-II code as,

$$\varphi_m = \tan^{-1} (1 - \mu_m^2 - \eta_m^2)^{1/2} / \eta_m, \quad \eta_m > 0 \quad (8)$$

$$\varphi_m = \tan^{-1} (1 - \mu_m^2 - \eta_m^2)^{1/2} / \eta_m + \pi, \quad \eta_m > 0 \quad (9)$$

According to the program, scattering transfer probability is also assumed to be represented by finite Legendre polynomial expansion as given below,

$$\sum_s = \sum_{n=0}^{\text{ISCT}} (2n+1)\sigma_{sn}(E' \rightarrow E) \sum_{k=0}^n R_n^k(\mu, \varphi) \Phi_n^k \quad (10)$$

And, the total source is given as S_{gijm} by the sum of,

$$(\text{SS})_{gijm} = (\text{Scatter source})_{gijm} = \sum_{h=1}^{\text{IGM}} \sum_{n=0}^{\text{ISCT}} (2n+1)\sigma_{snh \rightarrow g} \sum_{k=0}^n R_{mm}^k N_{nhij}^k$$

$$(\text{FS})_{gijm} = (\text{Fission source})_{gijm} = \chi_g \sum_{h=1}^{\text{IGM}} \nu \sigma_{fh} N_{0hij}^0 \quad (11)$$

$$(\text{IS})_{gijm} = (\text{Inhomogeneous source})_{gijm} = \sum_{n=0}^{\text{IQAN}} (2n+1) \sum_{k=0}^n R_{nm}^k Q_{ngij}^k$$

Where,

IGM: number of groups used,

ISCT: scattering order,

IQAN: distributed sources anisotropy order.

Although the S_N method has some advantages to solve transport equation, sometimes for some regions having strong absorbers and localized neutron sources some unexpected problems have been met; such as ray-effect. The ray-effect distortions that plague the method are anomalous ripples that appear in the scalar flux in two or three dimensional problems. These nonphysical bumps can be confused with physical ones, especially in deep penetration applications [4-5]. Nowadays, several remedies for eliminating or mitigating that problem have been proposed. It seems that the practical remedy for the ray-effect is to increase the order of S_N method (the number of directions). In general when this is done, the frequency of oscillations becomes higher and the magnitude becomes smaller. However, while substantial improvement results, ray-effects tend to be remarkably persistent even for high order S_N approximations [2,6].

3. RESULTS OF THE STUDY

In this study, to demonstrate the effects of cross-sections on the ray-effect, one of important two dimensional transport codes, TWOTRAN-II has been chosen and executed for two test problems. Problem 1 is a wellknown benchmark problem given in (x-y) two dimensional cartesian geometry [7]. In this problem there is a flat isotropic source at the left bottom corner of a square region. The boundary conditions are given as reflective on the bottom and the left sides, and vacuum on the top and the right sides of the region (Fig. 1).

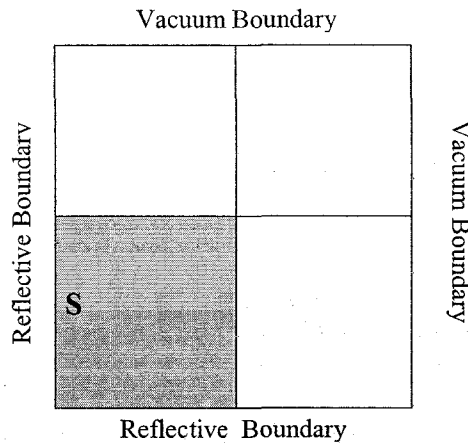


Fig.1: Sample problem in (x-y) geometry (Problem 1)

The parameters of problem 1 have been given in table 1. First, the code has been executed for this problem and distributions of scalar flux have been observed for $S_4 - S_{16}$ approximations. The ray-effect distortions in the flux have been examined by changing the values of scattering cross-section for each S_N approximation (Fig.2-4). Then, problem 1 has been adapted to cylindrical geometry (problem 2) and the effect of scattering cross-section on the ray-effect distortions has been examined in the similar way. The parameters of the problem 1, given in table 1, are also valid for the second problem, and the boundary conditions are taken to be the same. The results of problem 2 are demonstrated in figures (Fig.5-7).

$\Sigma_t = 1.0$		For both of problems
$\Sigma_f = 0.0$		
$S = 1.0$		
Σ_a	Σ_s	Case
0.0	1.0	4
0.25	0.75	1
0.50	0.50	2
0.75	0.25	3
1.0	0.0	5

Table 1: Problem parameters for sample problems

According to the figures obtained from problem 1, the case 4 which represents the scattering medium, is the best of all cases. It does not exhibit any ray-effect as expected [8,9]. Among the other cases, case 1 seems better than the others. If we compare all S_N approximations used in case 1, we observe that the S_4 approximation gives ray-effect. But, as the order of S_N approximations is getting higher a considerable mitigation is obtained. Because, in the low order S_N approaches, such as S_4 , the number of characteristic discrete directions allowed for particle streaming is restricted. Consequently, streaming contributions to the flux at a given position in the medium are limited to contributions from those characteristic directions in which source are visible. On the other hand, although the graph magnitude is reduced, the S_{16} graph seems better than the other graphs. Because in this approximation, according to the program, the number of characteristic directions used is given as 36 directions. These directions are calculated according to the relation given below.

$$MM = (ISN) * (ISN+2)/8$$

Where,

MM: number of directions per octant

ISN: order of S_N approximation

Besides, the case 5 which is a purely absorbing medium, is the worst of all cases as expected. In such medium a poor value of scalar flux is obtained no matter how many discrete directions are used.

Except for the magnitude of flux, this conclusion mentioned above is also valid for (r-z) cylindrical geometry (for problem 2) as seen in the figures, Fig.5, Fig.6 and Fig.7.

4. CONCLUSION

In this study, we tried to observe the ray-effect distortions depend upon the values of scattering and absorption cross-sections, by using two benchmark problems. We chose the best and the worst cases of all used in the study. We used different S_N approximations, such as S_4 , S_8 , S_{10} , S_{16} for each case as seen in the figures. By comparing these figures obtained from two problems we tried to make a conclusion about “the best” and “the worst” cases. But, the study mentioned here has not been completed yet. This article may be the first chapter of the whole study. For further study, we are planning to examine different boundary conditions for these problems. After completed all the examinations we planned, we will try some remedies to eliminate or strongly mitigate the ray-effect.

In this study, for the iteration count comparisons, no acceleration method was used to speed up convergence. This work has been operated by linux computer system.

Acknowledgments

The author is grateful to İstanbul Technical University staff for computer support.

References

- [1] R.D.O'dell and R.E.Alcouffe, Transport Calculations for nuclear analysis: Theory and guidelines for effective use of transport codes, *Los Alamos Lab.Report*, LA-10983, (1987).
- [2] E.E.Lewis and W.F.Miller Jr., *Computational Methods of Neutron Transport*, John Wiley and Sons Publ., (1984).
- [3] J.H.Mathews, *Numerical Methods for Mathematics, Science and Engineering*, Prentice Hall Int. Inc., (1992).
- [4] K.D.Lathrop and F.W. Brinkley, TWOTRAN-II: An Interfaced Exportable Version of the Twotrans Code for Two Dimensional Transport, *Los Alamos Scientific Lab.Report*, (1973).
- [5] J.E.Morel, T.A.Wareing, R.B.Lowrie, and D.K.Parsons, Analysis of Ray-Effect Mitigation Techniques, *Nucl.Sci.Eng.*, 144, (2003), 1.
- [6] V.Khromov, E.Kryuchh, G.Tikhomirov, L. Concharov and, V.Kondakov, *Nucl.Sci.Eng.*, 121, (1995), 264.
- [7] E.M.Gelbard, Benchmark Problem S-A1, *Argonne Code Center Benchmark Problem Book*, ANL-7416, Suppl. 1, Argonne National Lab, (1972).
- [8] T.Noh, W.F. Miller Jr., and J.E. Morel, *Nucl.Sci.Eng.*, 123, (1996), 38.
- [9] R.S. Baker, and K.R.Koch, *Nucl.Sci.Eng.*, 128, (1998), 312.

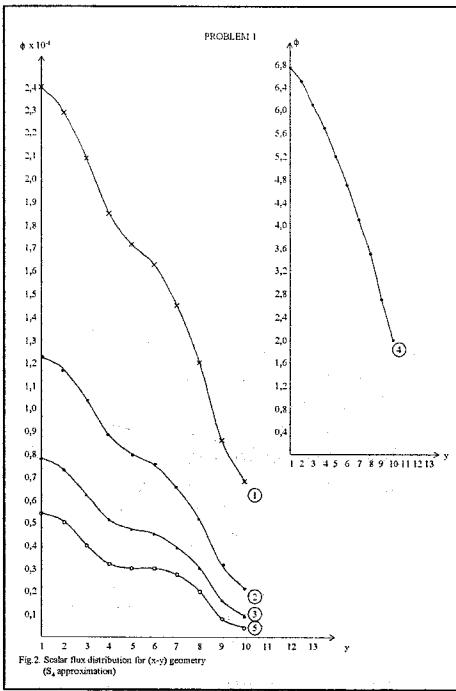


Fig.2. Scalar flux distribution for (x-y) geometry (S_4 approximation)

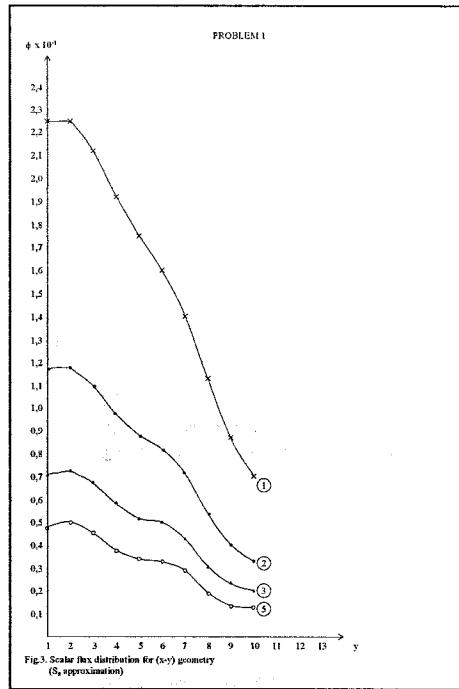


Fig.3. Scalar flux distribution for (x-y) geometry (S_8 approximation)

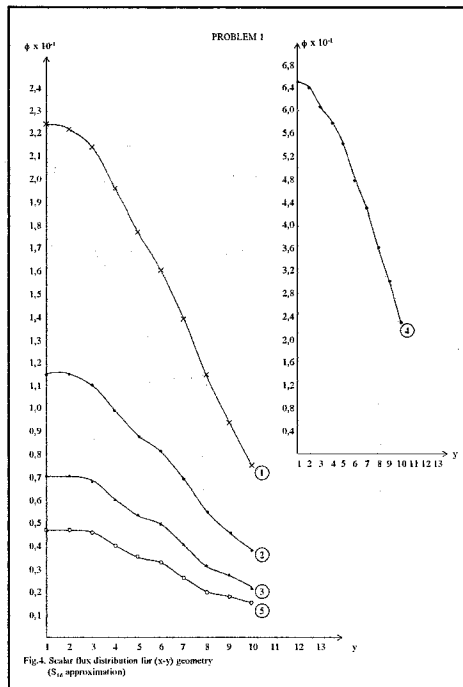


Fig.4. Scalar flux distribution for (x-y) geometry (S_{16} approximation)

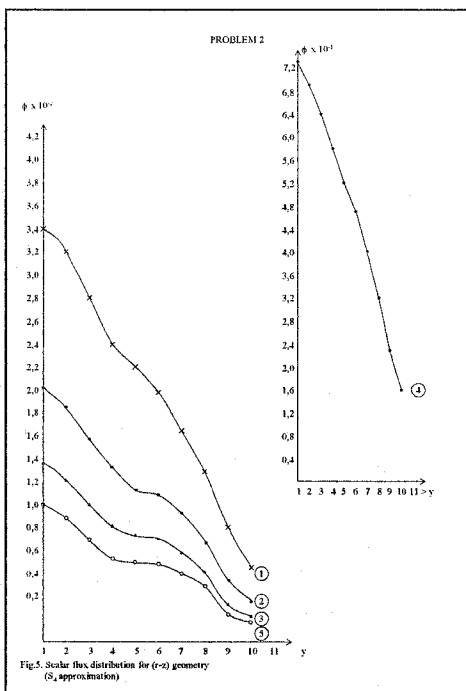


Fig.5. Scalar flux distribution for (r-z) geometry (S_4 approximation)

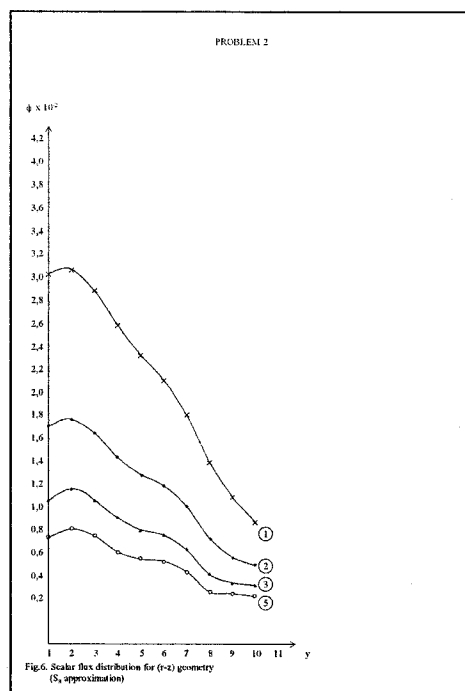


Fig.6. Scalar flux distribution for (r-z) geometry (S_8 approximation)

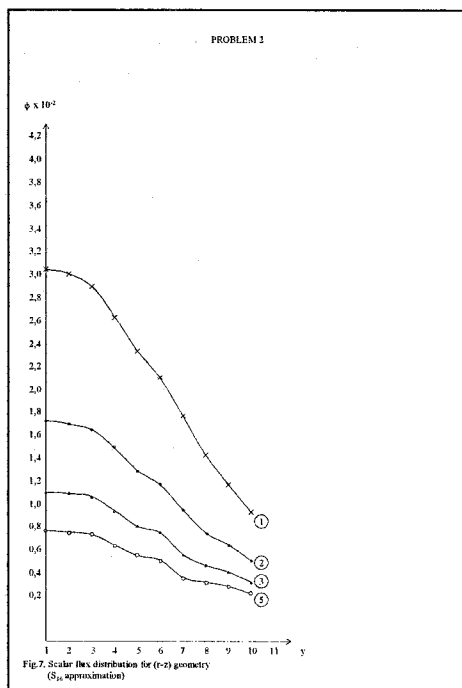


Fig.7. Scalar flux distribution for (r-z) geometry (S_{16} approximation)

Keywords

Neutron transport equation
Discrete Ordinates Method
Gauss-Legendre quadrature
Ray-effect distortions
Benchmark problems

List of Tables

Table 1. Problem parameters for sample problems

List of Figures

- Fig.1. Sample problem in (x-y) geometry (Problem 1)
- Fig.2. Scalar flux distribution for (x-y) geometry (S_4 approximation)
- Fig.3. Scalar flux distribution for (x-y) geometry (S_8 approximation)
- Fig.4. Scalar flux distribution for (x-y) geometry (S_{16} approximation)
- Fig.5. Scalar flux distribution for (r-z) geometry (S_4 approximation)
- Fig.6. Scalar flux distribution for (r-z) geometry (S_8 approximation)
- Fig.7. Scalar flux distribution for (r-z) geometry (S_{16} approximation)